LBL-34008
UC-413

Lawrence Berkeley Laboratory
UNIVERSITY OF CALIFORNIA

Presented at the Ninth Winter Workshop on Nuclear Dynamics,
Key West, Florida, January 31–February 5, 1993, and to
be published in the Proceedings

Complex Fragment Production and Multifragmentation in 60 MeV/u ^{129}Xe-Induced Reactions

G.J. Wozniak, W. Skulski, K. Tso, N. Colonna, and L.G. Moretto

April 1993

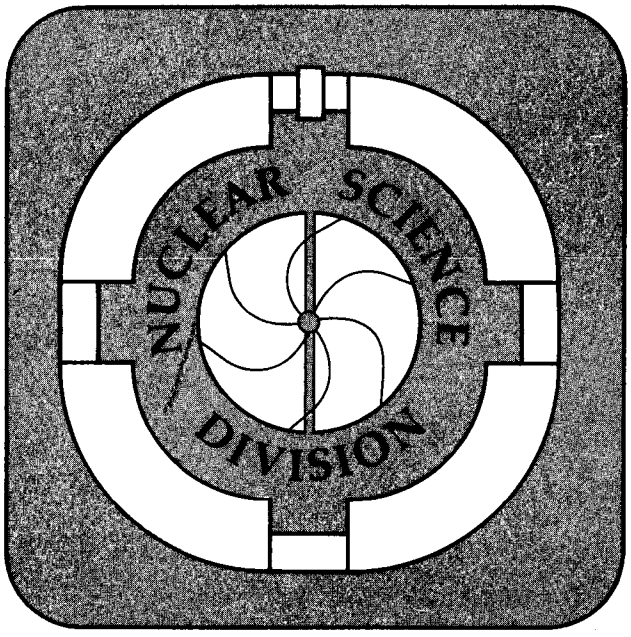

Prepared for the U.S. Department of Energy under Contract Number DE-AC03-76SF00098

DISCLAIMER

LBL - 34008

COMPLEX FRAGMENT PRODUCTION AND MULTIFRAGMENTATION IN 60 MeV/u ^{129}Xe-INDUCED REACTIONS

G. J. Wozniak, W. Skulski, K. Tso, N. Colonna and L. G. Moretto

Nuclear Science Division, Lawrence Berkeley Laboratory
University of California, Berkeley, California 94720, USA

April, 1993

This work was supported by the Director, Office of Energy Research, Division of Nuclear Physics of the Office of High Energy and Nuclear Physics of the U.S. Department of Energy under Contract DE-AC03-76SF00098

COMPLEX FRAGMENT PRODUCTION AND MULTIFRAGMENTATION IN 60 MeV/u ^{129}Xe-INDUCED REACTIONS

G. J. WOZNIAK, W. SKULSKI, KIN TSO, N. COLONNA and L. G. MORETTO
Nuclear Science Division, Lawrence Berkeley Laboratory,
1 Cyclotron Road, Berkeley, CA 94720

ABSTRACT

Complex fragment production has been studied in nearly 4π geometry for the 60 MeV/u ^{129}Xe + ^{27}Al, ^{nat}Cu, ^{89}Y, ^{165}Ho and ^{197}Au reactions. The total number of light charged particles and complex fragments increases strongly with the mass of the target, reaching values of 40 for the ^{197}Au target. The yield of intermediate mass fragments reaches values greater than 10 for central collisions on ^{197}Au. For a subset of the events, 80% of the total charge in the reaction channel is detected.

1. Introduction

Multifragmentation is one of the most striking processes observed in intermediate-energy heavy-ion reactions[1-12]). In the bombarding energy range of 30 - 100 MeV/u, complex fragments are produced in abundance. In central collisions with heavy projectiles, complete disassembly of the nuclear system into nucleons and light fragments has been observed. In peripheral collisions, excited projectile-like and target-like remnants are observed. For bombarding energies at the lower end of this range, deep-inelastic-like collisions were observed even for central collisions[13]).

The yield of multifragment events has been shown to increase strongly with increasing excitation energy[3, 11]). The excitation energy of the nuclear system can be increased by increasing the bombarding energy, however, pre-equilibrium emission limits the energy that can be deposited. An alternative method of increasing the excitation energy is to increase the target mass in reverse-kinematics reactions. Recent studies with 50 MeV/u ^{129}Xe projectiles on targets ranging from ^{12}C to ^{197}Au showed a strong increase in both the light charged particle and intermediate mass fragment (IMF) multiplicities with increasing target mass. The large production of IMFs from the ^{197}Au target has posed a severe challenge for many models[1]). In the present work, we report on some early results on complex fragment production and multifragmentation from 60 MeV/u ^{129}Xe-induced reactions.

2. Experimental Technique

The experiment was performed at K1200 Cyclotron of the National Superconducting Cyclotron Laboratory at Michigan State University. A 60 MeV/u ^{129}Xe beam bombarded targets of ^{27}Al, ^{nat}Cu, ^{89}Y, ^{165}Ho and ^{197}Au. The detection system subtended angles from 2° to 160° with respect to the beam axis with a geometric acceptance of ~88% of 4π. At very forward angles (2° - 16°), fragments (Z = 1 - 54) were detected in a 16-telescope (Si-Si-Plastic) array[14]) with good energy and position resolution. At larger angles (16° - 160°), light charged particles and fragments (Z = 1 - 20) were detected in the MSU Miniball[15]). Representative detection thresholds in the forward array where 13, 21 and 27 MeV/u for fragments of

Z = 8, 20 and 54, respectively. In the Miniball, detection thresholds were 2, 3, and 4 MeV/u for Z = 3, 10, and 18 fragments, respectively.

3. Reaction Model

Extensive efforts have been made to describe intermediate-energy heavy-ion reactions in terms of kinetic equations. In these semiclassical approaches, the collisionless Vlasov equation has been augmented with a collision (Boltzmann) term. The incorporation of nuclear forces of the Skyrme type, plus an empirical Fermi potential to mock up the Pauli principle has led to a series of dynamical theories with various acronyms: Landau-Vlasov (LV), Boltzmann-Uehling-Uhlenbeck (BUU) or Boltzmann-Nordheim-Vlasov (BNV). There are some fundamental short comings in them, for example, the Pauli principle is not rigorously respected. Another shortcoming is the inability of these approaches to accurately describe the statistical decay in the long time limit. This has remedied by terminating the dynamical calculation at a suitable time, after energy relaxation has occurred, and continuing the calculation with a compound-nucleus decay code[16-18]) or a multifragmentation code[2, 4, 6, 7, 19-22]).

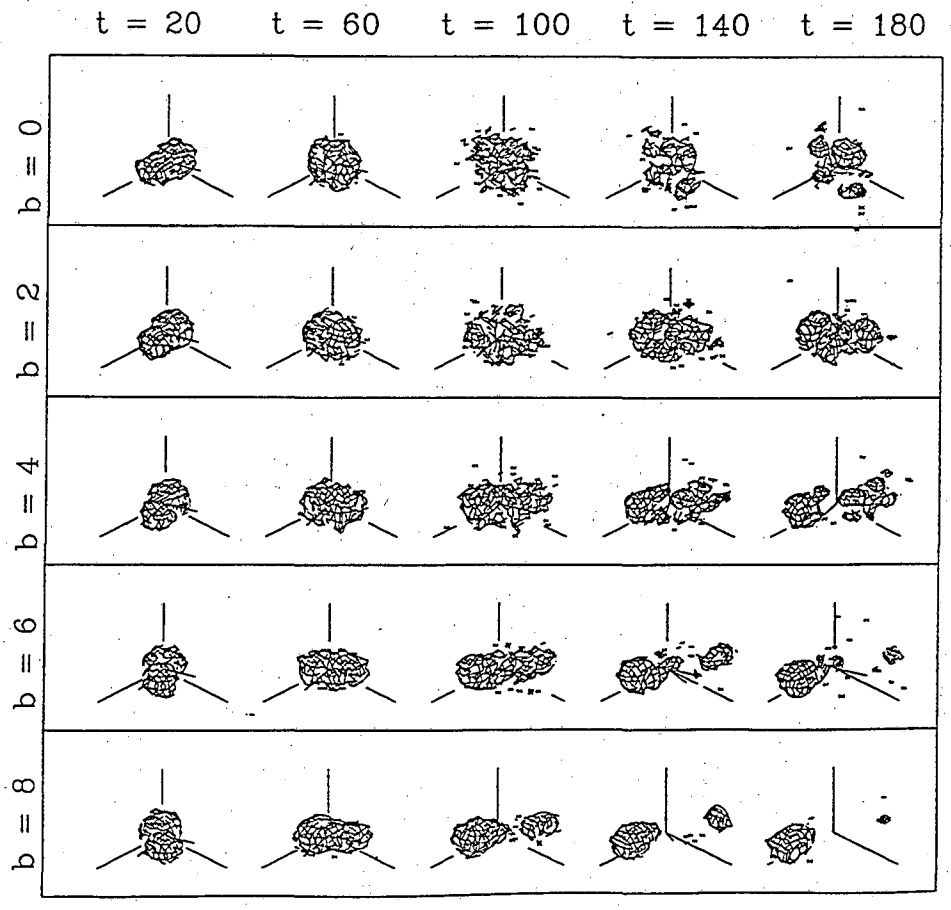

Fig. 1 BNV calculations of the time evolution of the reaction 60 MeV/u $^{129}Xe + {}^{nat}Cu$ reaction for several different impact parameters (b). The calculations were performed with an incompressibility constant of K = 200 MeV and 40 test particles/nucleon. Each row contains a different impact parameter and each column a different time step in units of fm/c.

Nevertheless, it is useful to use a reactions dynamics code to get an overview of the heavy-ion collision process. To examine the impact parameter dependence of fragment production, we have used a BNV simulation[16, 17]) of the 60 MeV/u ^{129}Xe + ^{nat}Cu reaction. For the most peripheral collisions (b = 6 to 8 fm), excited project-like and target-like fragments are produced. As the impact parameter decreases, the target-like fragment losses its identity and the forward going projectile-like fragment decreases in size. For the most central collisions, the system breaks up into several hot primary fragments that do not seem to be obviously related to either the projectile or the target.

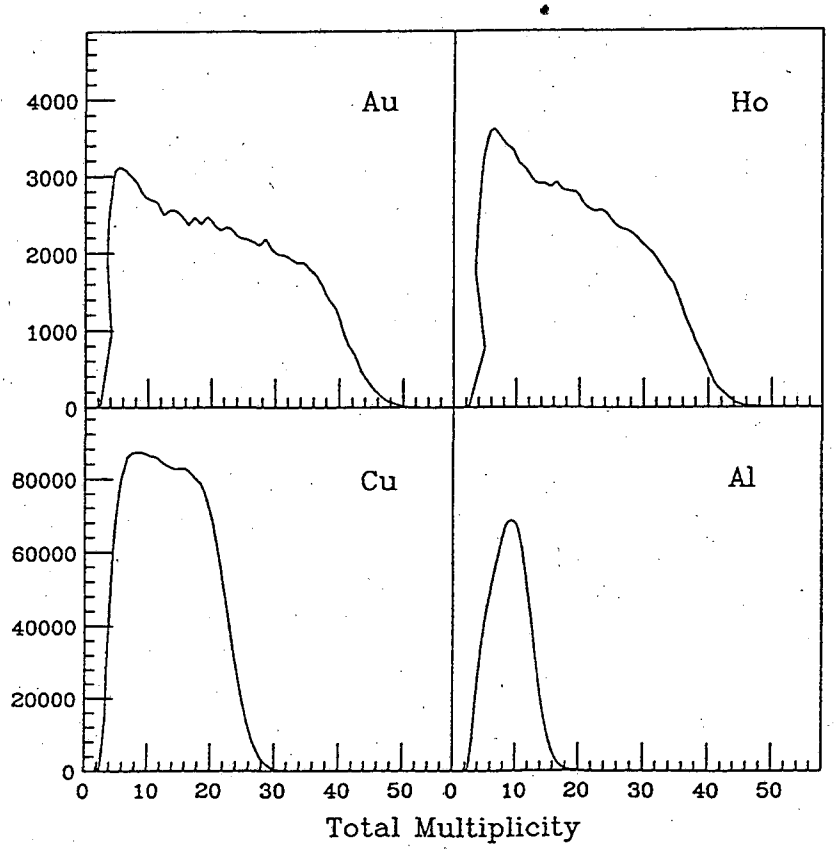

Fig. 2. Measured charged-particle multiplicity distributions for 60 MeV/u Xe-induced reactions on four different targets. Each panel contains a distribution for a different target.

4. Experimental results

As the excitation energy of a compound nucleus is increased, one would expect the evaporation of neutrons and light charged particles to increase. If the excitation energy exceeds the binding energy of the nuclear system, one expects the system to disassemble into nucleons and light fragments. Thus, many groups have used 4π neutron or charged particle detectors to determine the extent to which the kinetic energy available in the entrance channel is thermalized. In fact recent

measurements[13]) that combine both detection techniques have shown a strong correlation between the neutron and charged particle multiplicity.

In our measurements, we utilize the total number of charged particles detected M_n which consists of the measured number of light charged particles, intermediate mass fragments, and unidentified hits. Figure 2 shows how M_n depends on the target mass for 60 MeV/u ^{129}Xe-induced reactions. As the target mass is increased, the distribution broadens and the maximum value increases dramatically. For the ^{197}Au target, up to 40 particles were detected. The available center-of-mass (c.m.) energy is lowest for the asymmetric ^{129}Xe + ^{27}Al reaction and relatively small values of M_n are observed. As the target mass is increased, the available c.m. energy and M_n increase indicating that more kinetic energy is being thermalized. The distributions broaden for the heavy targets due to the larger range of impact parameters that result in charged particle emission.

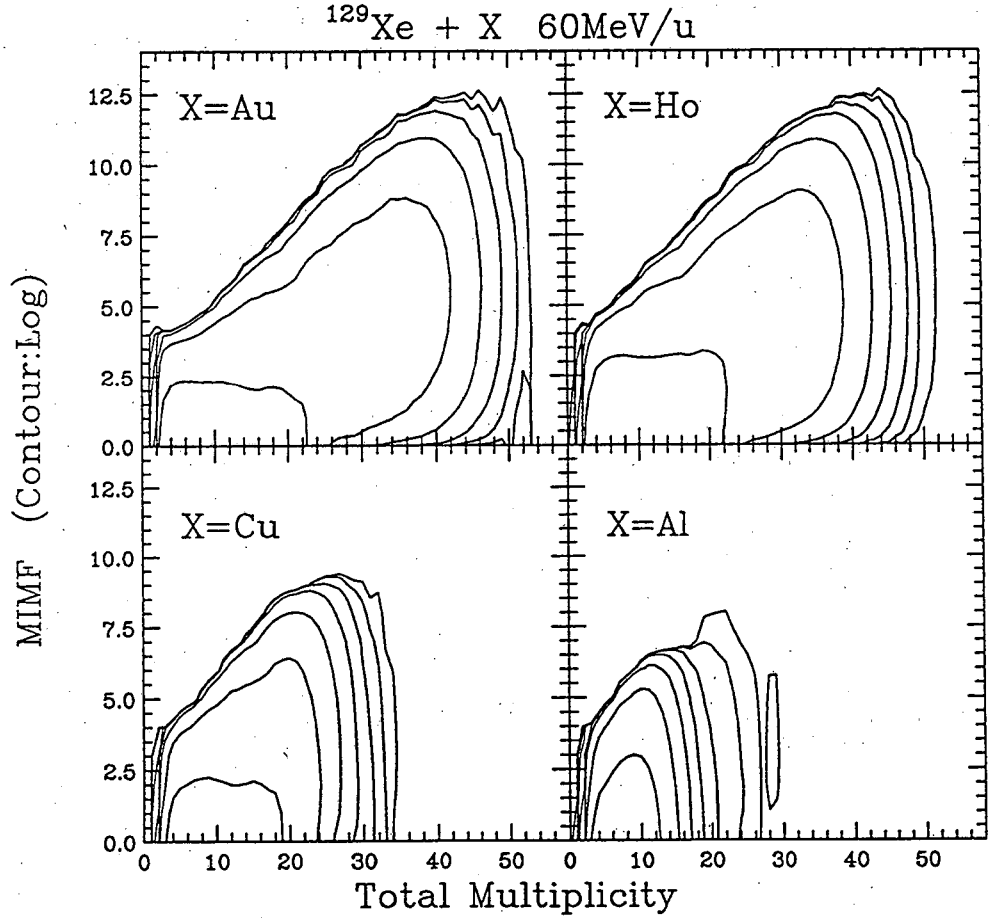

Fig. 3 Logarithmic contour plots showing the relationship between N_{IMF} and N_Z. Each panel contains a different target. Each succeeding contour corresponds to a factor of 10 increase in yield.

It is interesting to determine how the number of intermediate mass fragments correlates with the total charged particle multiplicity (see Fig. 3). For each projectile-target combination, N_{IMF} increases with M_n. Larger fragment multiplicities are

observed for reactions on the heavier targets that have larger c.m. energies and more mass available. More than 10 intermediate mass fragments are observed for the highest values of M_n.

For the ^{27}Al target, M_n is 10 whereas values up to 40 charged particles are observed for the ^{197}Au target. Since the total charge of these two systems is 67 and 133, an obvious question is how much of the total system charge has been detected. This is a relevant question, because we do not have an ideal detector with perfect 4π coverage and zero detection thresholds. In particular, the slow moving target-like fragments are very difficult to detect and identify.

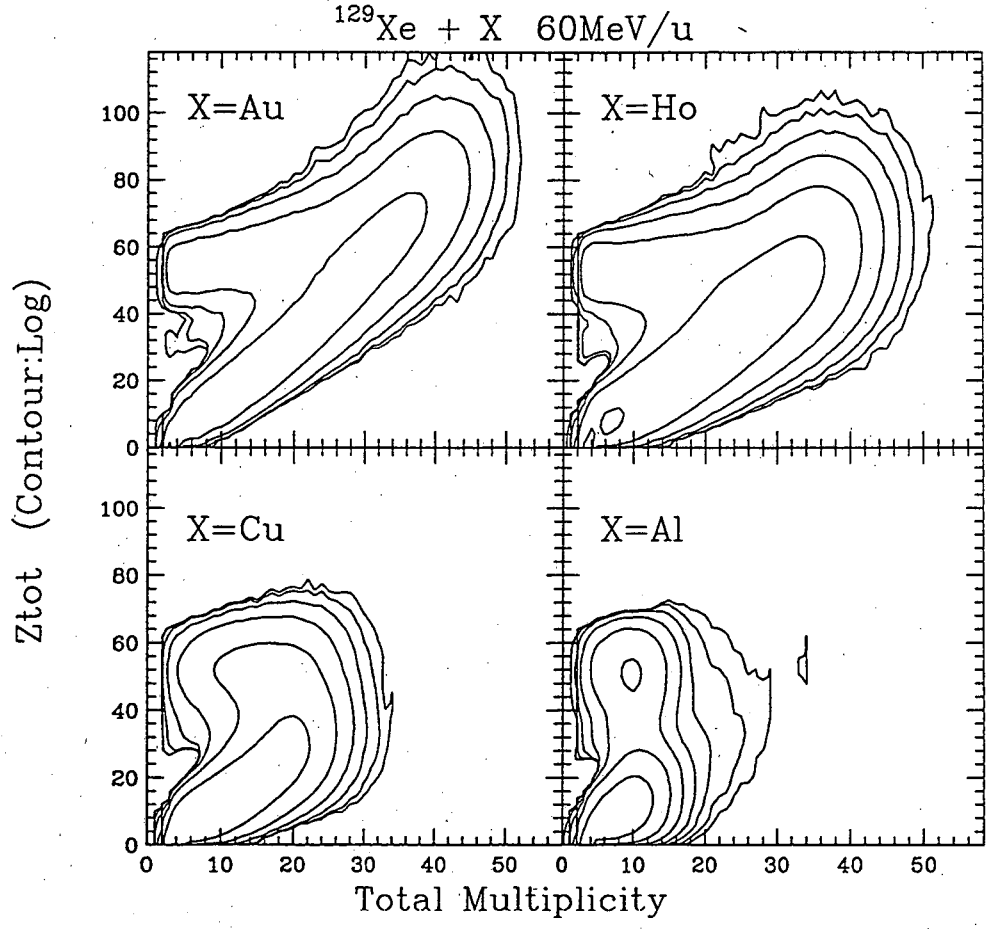

Fig. 4 Logarithmic contour plots showing the total charge detected and the total charge multiplicity. Each panel contains a different target. Each succeeding contour corresponds to a factor of 10 increase in yield. The fact that some charged particles are not identified, but counted in the total multiplicity causes some events to fall below the diagonal.

Figure 4 shows a comparison of the total detected charge versus the total number of detected particles M_n for the four different targets. For the very asymmetric system $^{129}Xe + ^{27}Al$, the distribution has two peaks. The higher peak has a Z_{total} of ~50 and the lower one a Z_{total} of 10. For the upper peak, 90% of the total charge of the system is detected, whereas for the lower peak, only a small percentage is detected. The lower peak corresponds to the situation when the heavy projectile-like fragment is not

detected due either to it being emitted into an angle smaller than 2° or the dead region between telescopes. When the heavy forward-going fragment is not detected, one sees only light particles emitted from the target and projectile-like residues.

For heavier targets, one observes two branches. For small values of N_Z, the upper branch starts at the projectile Z-value. As the total particle multiplicity increases, this branch is roughly constant and then joins the lower branch. For the most central collisions, total detected number of charged particles is larger than the projectile charge. The two-branch region can be associated with peripheral collisions: the lower branch arises when the forward going projectile-like fragment is missed and only light-charged particles have been detected; whereas the upper branch results when both of these are detected. In this region, one does not detect the total charge of the system because the slow moving target-like fragment is below the detector thresholds. One can interpret this pattern as follows, as the impact parameter decreases, the target-like fragment becomes more excited and emit increasing numbers of light charged particles causing the lower branch to increase until the two branches merge. For the most central collisions, the system breaks into many small fragments and no large projectile-fragment remains. A very similar pattern is observed in plots of the total kinetic energy detected versus the total multiplicity (see Figure 5).

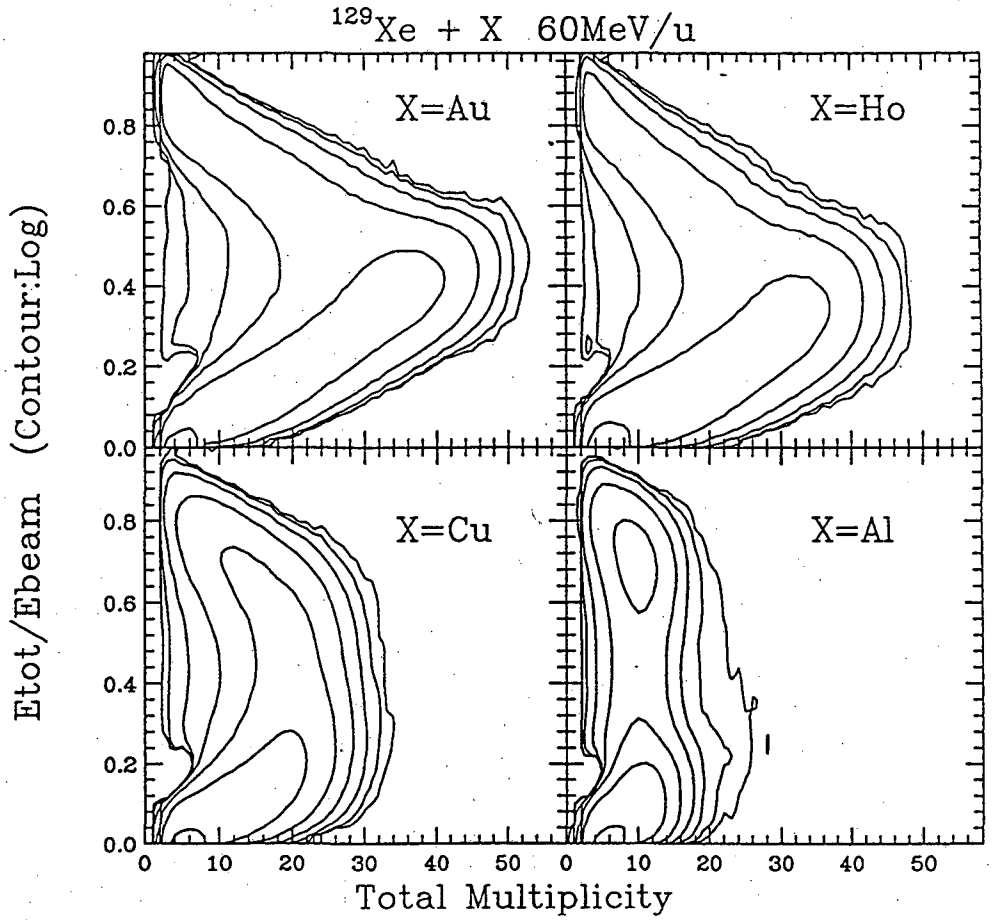

Fig. 5 Logarithmic contour plots showing the total kinetic energy detected and the total charge multiplicity. Each panel contains a different target. Each succeeding contour corresponds to a factor of 10 increase in yield.

5. Conclusion

A preliminary analysis of the 60 MeV ^{129}Xe-induced reactions shows the power of 4π measurements and the need to measure the products emitted at very forward angles. In particular, for intermediate-energy reactions with heavy projectiles, a large fraction of the total mass (charge) is emitted at forward angles due to the kinematics of the reaction.

6. Acknowledgments

We would like to acknowledge our MSU collaborators who participated in the acquisition of these data: D. R. Bowman, M. Chartier, C. K. Gelbke, W. C. Hsi, M. A. Lisa, W. G. Lynch, G. F. Peaslee, L. Phair, C. Schwarz, and M. B. Tsang

This work was supported by the Director, Office of Energy Research, Division of Nuclear Physics of the Office of High Energy and Nuclear Physics of the US Department of Energy under contract DE-AC03-76SF00098.

7. References

1) D. R. Bowman, et al., *Phys. Rev. Lett.* **67** (1991) 1527.
2) D. R. Bowman, et al., *Phys. Rev.* **C46** (1992) 1834.
3) Y. Blumenfeld, et al., *Phys. Rev. Lett.* **66** (1991) 576.
4) K. Hagel, et al., *Phys. Rev. Lett.* **68** (1992) 2141.
5) J. Hubele, et al., *Z. Phys.* **A340** (1991) 263.
6) J. Hubele, et al., *Phys. Rev.* **C46** (1992) R1577.
7) P. Kreutz, et al., *Nucl. Phys.* A (1993).
8) C. A. Ogilvie, et al., Phys. Rev. Lett **67** (1991) 1214.
9) E. Piasecki, et al., Phys. Rev. Lett. **66** (1991) 1291.
10) L. Phair, et al., *Phys. Lett.* **B285** (1922) 10.
11) P. Roussel-Chomaz, *Nucl. Phys.* **A551** (1993) 508.
12) R. T. d. Souza, et al., *Phys. Lett.* **B268** (1991) 6.
13) B. Lott, et al., *Phys. Rev. Lett.* **68** (1992) 3141.
14) W. L. Kehoe, et al., *Nucl. Instr. Meth. Phys. Res.* **A311** (1992) 258.
15) R. T. d. Souza, et al., *Nucl. Instr. and Meth.* **A295** (1990) 109.
16) M. Colonna, et al., *Phys. Lett.* **B283** (1992) 180.
17) M. Colonna, et al., *Nucl. Phys.* **A541** (1992) 295.
18) M. Blann and M. G. Mustafa, *Phys. Rev.* **C44** (1991) R590.
19) H. W. Barz, et al., *Phys. Rev.* **C46** (1992) R42.
20) S. Leray, et al., *Nucl. Phys.* **A511** (1990) 414.
21) S. Leray, et al., *Nucl. Phys.* **A531** (1991) 177.
22) B.-A. Li, A. R. DeAngelis and D. H. E. Gross, Hahn-Meitner-Institut Berlin GmbH (1993).

LAWRENCE BERKELEY LABORATORY
UNIVERSITY OF CALIFORNIA
TECHNICAL INFORMATION DEPARTMENT
BERKELEY, CALIFORNIA 94720